Friction stabilities of gypsum and kaolinite/calcite mixture fault gauges under high pressure

Dongsheng Ren*

State Key Laboratory of Earthquake Dynamics, Institute of Geology, China Earthquake Administration, Beijing, China

Various lab-scale friction tests and seismic observations have highlighted the role of fault gauges in earthquake initiation in geological faults. These fault gauges consist of particles accumulated over thousands of years due to surface wear caused by friction. Understanding their properties is crucial as they significantly influence both the frictional strength and sliding stability of faults. This study investigates the friction stability parameter (a–b) under loading rates of 0.2−25 µm/s using velocity step tests on gypsum fault gauges under a low normal stress condition (0.9 MPa) and steady-state velocity step tests on fault gauges composed of varying ratios of kaolinite/calcite mixture under an effective normal stress of 3 MPa. The conclusions drawn from this study are as follows: 1) The (a–b) values obtained from near steady-state velocity step tests on gypsum fault gauges and those reported in previous studies under similar conditions were both negative. However, our results show that the former values were one order of magnitude lower than the latter, indicating a higher susceptibility to velocity weakening. 2) Steady-state velocity step tests on the kaolinite/calcite mixture fault gauges demonstrated positive (a–b) values for all mixtures with varying kaolinite contents. Moreover, the (a–b) values were proportional to the kaolinite content. We established a functional relationship between the (a–b) values of the mixture fault gauge and the mass fraction of kaolinite, providing valuable insights for future experiments and numerical simulations related to fault stability.
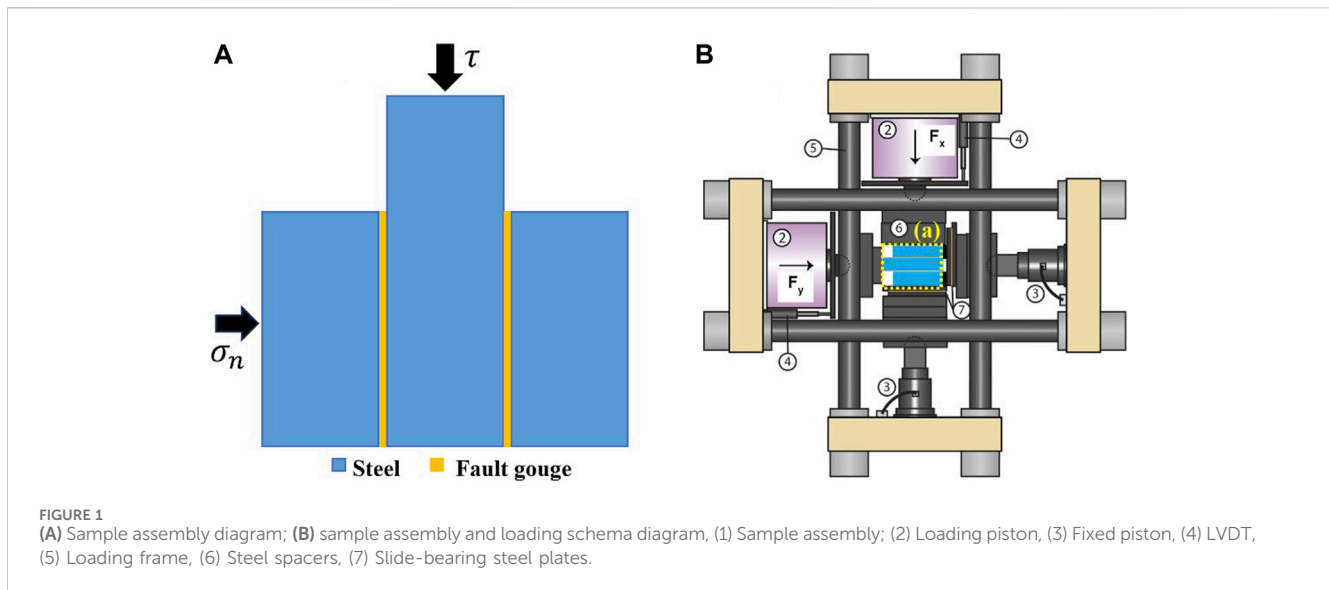
KEYWORDS

friction stabilities, gypsum, kaolinite/calcite mixture, high pressure, fault gauges

1 Introduction

Earthquakes are natural phenomena resulting from abrupt accelerated sliding on tectonic faults. This sliding releases energy through seismic waves and heat (Niemeijer et al., 2012). Seismic waves propagate through the earth's crust, causing surface vibrations, and earthquakes with significant magnitudes can result in substantial loss of life and property. Therefore, comprehending earthquake formation processes and mechanisms has become a relentless pursuit for numerous scientific researchers (Scholz, 1989; He et al., 1998; Marone, 1998; Mair et al., 2002; West et al., 2005; BenDavid et al., 2010; Kaproth and Marone, 2013). Brace and Byerlee (1966) introduced one crucial understanding of earthquake mechanisms, who suggested that the stick-slip phenomenon observed during the relative sliding of two rocks in laboratory experiments might be a mechanism for shallow earthquakes.

Since then, extensive laboratory friction experiments have been conducted to investigate the sliding properties of rock-rock interfaces (Johnson and Scholz, 1976; Scholz and Engelder, 1976; Engelder, 1978; Dieterich, 1979; Lockner and Okubo, 1983; Weeks and

FIGURE 1
(A) Sample assembly diagram; **(B)** sample assembly and loading schema diagram, (1) Sample assembly; (2) Loading piston, (3) Fixed piston, (4) LVDT, (5) Loading frame, (6) Steel spacers, (7) Slide-bearing steel plates.

Tullis, 1985; Tullis, 1988; Kato et al., 1992; Karner and Marone, 2000). Nevertheless, lab-scale friction tests and seismic observations revealed that fault gauges in geological faults may play a critical role in earthquake initiation. These fault gauges consist of particles accumulated through surface wear over thousands of years due to friction.

The properties of fault gauges have a decisive influence on both the frictional strength and sliding stability of faults (Brace and Byerlee, 1966; Johnson et al., 1973; Sammis and Biegel, 1989; Frye and Marone, 2002; Mair et al., 2002; Anthony and Marone, 2005; Marone et al., 2008; Ikari et al., 2015; Scuderi et al., 2015; Jiang et al., 2016; Lieou et al., 2017; Hedayat et al., 2018). However, acquiring natural deep fault gauges without compromising their micromorphs and loading history is nearly impossible. To study the sliding properties of fault gauges, some scholars have used fault gauge samples collected from outcrops of fault surfaces (He et al., 2007). Various granular materials have also been used as simulants for fault gauges, assembled into the sliding surface of simulated faults in laboratories. These include pulverized particles obtained by manually grinding various rocks (Byerlee, 1978; Engelder, 1978; Morrow and Byerlee, 1989; Moore et al., 1997; He et al., 2007; Togo et al., 2011; Lu and He, 2014), industrially produced granular materials like finely ground glass beads (Géminard et al., 1999; Albert et al., 2001; Adjemian and Evesque, 2004; Härtl and Ooi, 2008; Johnson et al., 2013; Lastakowski et al., 2015; Rivière et al., 2018), MgO nanoparticles (Han et al., 2011; Yao et al., 2016), and even kitchen flour (Shinbrot et al., 2012; Leeman et al., 2015).

Within the framework of the rate- and state-dependent friction criterion, velocity weakening is a necessary condition for earthquakes to occur, while velocity strengthening typically cannot cause earthquakes (Scholz, 1998). Recent studies have shown that on some naturally seismogenic faults, creep on the fault during the seismic gap is unevenly distributed across the fault (Freymueller et al., 2000; Chlieh et al., 2008). This means that while some areas inside the fault are self-locking and undergoing stress recovery to prepare for the next earthquake, others are slowly creeping. These observations suggest the simultaneous existence of speed enhancement and velocity

weakening on the same fault. In laboratory settings, some scholars have explored the influence of material inhomogeneity on fault belts' sliding properties (Buijze et al., 2021; Bedford et al., 2022). Consequently, investigating the friction stability of fault gauges with different attributes greatly aids related research on laboratory earthquakes. Prior studies have indicated that gypsum behaves as a speed-weakening material at room temperature (Buijze et al., 2021), meaning that (a-b) < 0. As such, (a-b) of gypsum is fitted through stick-slip experiments and cannot be obtained by steady-state tests of speed steps. Conversely, calcite and kaolinite are velocity-enhanced materials at room temperature (Buijze et al., 2021), signifying that (a-b) > 0. However, the friction properties of their mixtures have not been systematically reported to date. Given these reasons, it holds significant scientific importance to study the changes in friction stability parameters (a-b) through velocity step tests of gypsum fault gauges under low normal stress conditions and steady-state tests of speed steps of kaolinite/calcite mixture fault gauges with different proportions.

2 Experimental

The experiment was conducted at the Structural Physics Laboratory of the Institute of Geology, China Earthquake Administration. Gypsum, calcite, and kaolinite were purchased from Aladdin Company. We controlled the particle size of the gypsum fault gauge to 100–150 μm and that of kaolinite and calcite to 75–100 μm through grinding and sieving. To enhance the rigidity of the entire system and promote stable fault sliding, we used steel blocks for the surrounding rock of the fault. The steel blocks on both sides measured $100 \times 50 \times 50$ mm³, while the middle steel block measured $150 \times 50 \times 50$ mm³. The thickness of the fault gauge was 1.5 mm. Figure 1A shows the specific sample loading mode. Initially, we placed the assembled samples on the horizontal biaxial press, which had a maximum single-axis load capacity of 150 t and could be driven by either displacement or load control. We first loaded pressure in the F_x direction to the predetermined pressure, which was
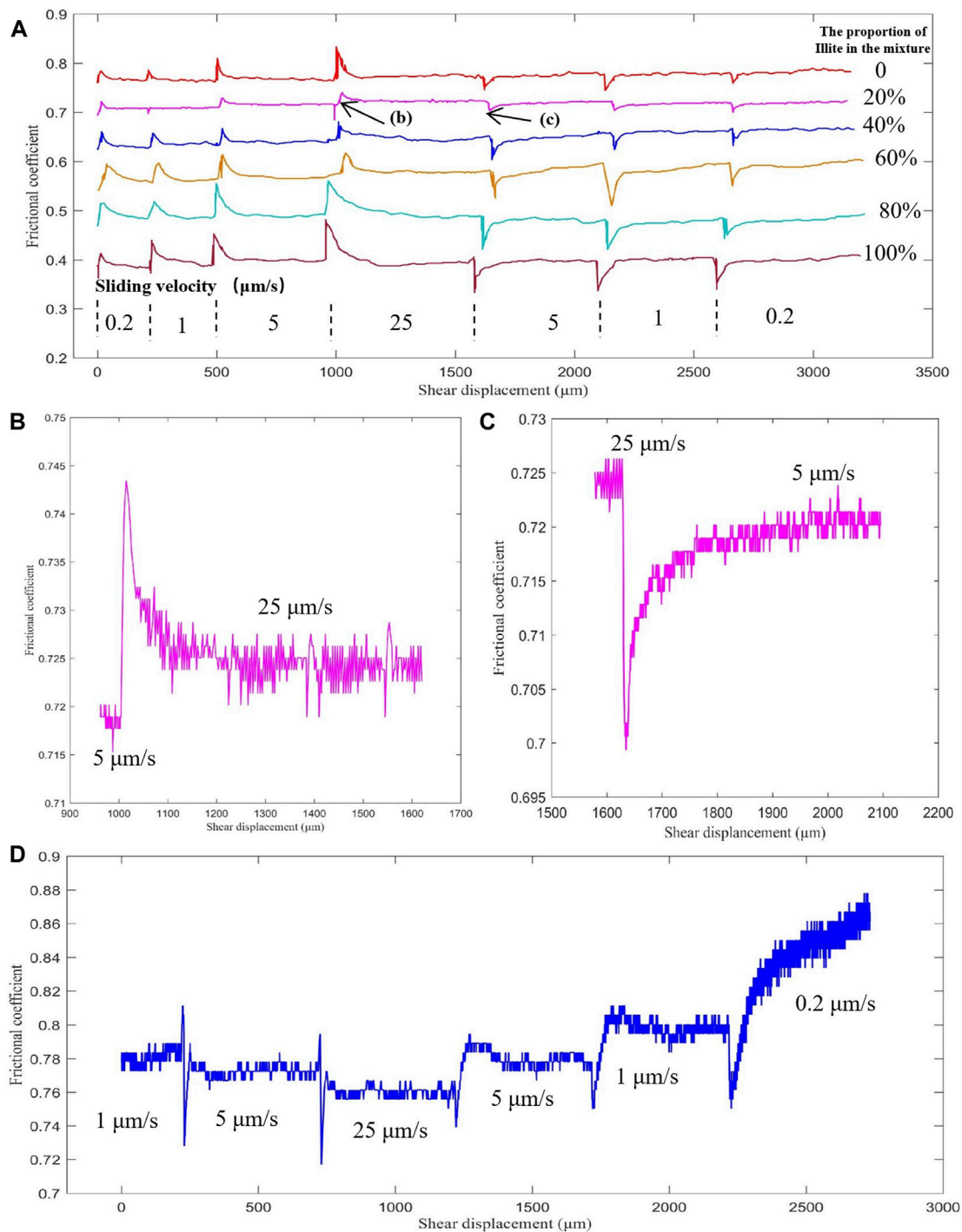
FIGURE 2
(A) Curves of the fault gauge frictional coefficient changing with displacements of different proportions of kaolinite/calcite mixture under the condition of room temperature and 3 MPa effective normal stress, **(B)** and **(C)** enlarged images of the black arrow in **(A)**, **(D)** variation curve of gypsum fault gauge frictional coefficient with displacement under the condition of room temperature and 0.9 MPa effective normal stress.

0.9 MPa for the gypsum fault gauge experiment and 3 MPa for the kaolinite/calcite mixture experiment. Once the F_x direction reached the predetermined pressure, we controlled the F_y direction using displacement and performed shear experiments at speeds of 0.2, 1, 5, and 25 μm/s, allowing approximately 0.5 mm of slip under each speed condition until the sliding reached a steady state.

After completing the experiment, we determined the values of the friction stability parameters (a-b) based on the rate-state friction constitutive relation. Rate- and state-dependent friction is described using τ and refers to the conditions under which materials either strengthen or weaken with an imposed velocity step (Dieterich, 1979; Ruina, 1983). The Dieterich-Ruina formulation allows us to
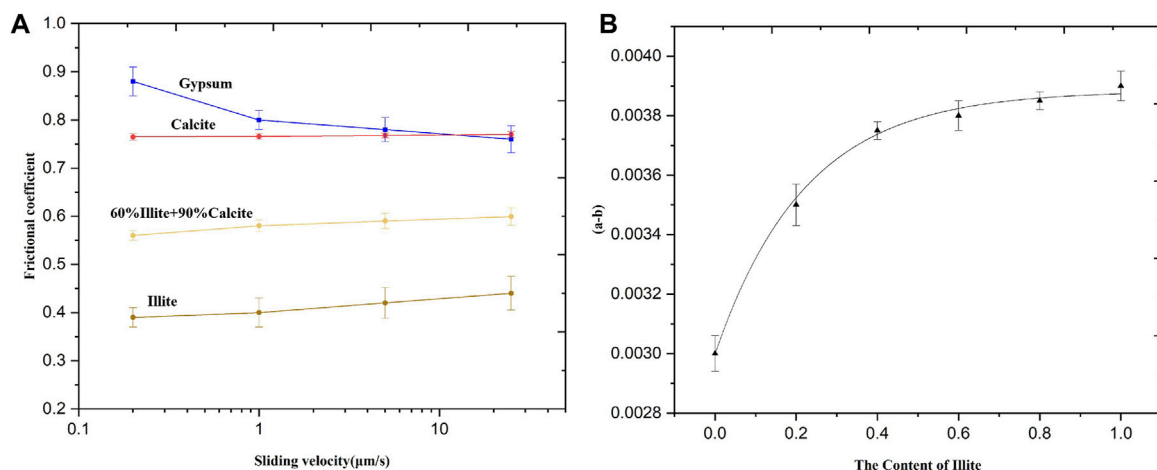
FIGURE 3
(A) Variation of frictional coefficient with loading rate for different fault gauge, **(B)** variation of kaolinite/calcite mixture fault gauge **(A, B)** with the mass fraction of kaolinite.

calculate τ as follows: τ $\tau = \sigma (\mu_0 + aln\frac{v}{v_0} + bln\frac{\theta v_0}{D_c})$, where σ represents the effective normal stress, and μ_0 is the friction coefficient when the slip velocity (V) equals the reference velocity (v_0). The direct effect term ($aln\frac{v}{v_0}$) accounts for the initial increase in frictional strength, while the evolution term ($bln\frac{\theta v_0}{D_c}$) accounts for the reduction in frictional strength with slip distance and time, where D_c denotes the critical slip distance, and θ denotes the state variable. The parameters a and b are empirical, dimensionless quantities that govern these terms. The term $(a - b)$ represents the velocity dependence of the material under specific environmental conditions, such as stress, temperature, slip velocity, and fluid effects (Marone, 1998). When the sliding reached a steady state, $(a - b) = \Delta\mu_s/\Delta Ln (V)$.

3 Results and discussion

Figure 2A illustrates the stable sliding behavior of different kaolinite/calcite mixtures under various loading rates (0.2–25 μm/s). As the proportion of kaolinite mass increases, the overall mixed fault gauge's frictional coefficient gradually decreases. The frictional coefficient exhibits sudden changes during the experimental loading rate switching process, where an increase in loading rate results in a sudden increase in the frictional coefficient (Figure 2B), and a decrease in loading rate leads to a sudden decrease in the friction coefficient (Figure 2C).

Previous studies suggested that gypsum exhibits stick-slip behavior under different normal stress conditions at room temperature (Buijze et al., 2021). However, using steel blocks as the surrounding rock and a low effective normal stress of 0.9 MPa in our experimental design is not conducive to stick-slip in the gypsum fault gauge. Therefore, we observe a more stable sliding behavior in the gypsum fault gauge. The accuracy of the gypsum fault gauge's (a-b) obtained through the steady-statevelocity steptest is superior to the value obtained by fitting the stick-slip data (Dieterich, 1979; Ruina, 1983). Additionally, the friction coefficient exhibits sudden changes during the experimental loading rate switching process,

where an increase in loading rate leads to a sudden decrease in the friction coefficient, while a decrease in loading rate causes a sudden increase.

Based on the data, we derived the variation curves of different fault gauge frictional coefficients with loading rate, as shown in Figure 3A. Using the formula $(a - b) = \Delta\mu_s/\Delta Ln (V)$, we determined that the slope of the curve in Figure 3 (middle) represents the (a-b) value of the fault gauge. The slope of the gypsum fault gauge is less than 0, indicating velocity weakening under this loading condition, with (a-b) approximately −0.01. Compared with the (a-b) value of −0.0031 (deMeer and Spiers, 1997) obtained through fitting the gypsum fault gauge under similar particle size conditions, our results show stronger velocity weakening. In contrast, the slopes of the kaolinite/calcite mixture fault gauges are all positive, indicating speed enhancement characteristics. Furthermore, as the kaolinite content increases, the slope of the curve becomes larger, suggesting that the (a-b) value of the material increases with the proportion of kaolinite. Additionally, we calculated the mixed fault gauge's (a-b) for different kaolinite content, as shown in Figure 3B. This allowed us to establish the relationship between the mixed fault gauge's (a-b) and kaolinite content. Through this relationship, we can estimate the mixed fault gauge's (a-b) for different kaolinite mass fractions, providing a basis for future experiments and numerical simulations.

4 Conclusion

By designing a well-designed steady-state velocity step test, we successfully determined the values of (a-b) for both the gypsum fault gauge and the fault gauge consisting of different components of the kaolinite/calcite mixture. For the gypsum fault gauges, the (a-b) values obtained through near steady-statevelocity steptests and those reported in previous studies under similar conditions were negative. However, the (a-b) values obtained in our tests were one order of magnitude lower than those reported in previous studies, indicating that the gypsum fault gauge in our experimental setup

exhibits a stronger tendency toward velocity weakening. Our steady-state velocity step tests on the kaolinite/calcite mixture fault gauges revealed that all mixtures, regardless of their kaolinite contents, exhibited positive (a-b) values. Furthermore, we observed a proportional relationship between (a-b) and the kaolinite content. As a result, we established a functional relationship between the (a-b) values of the mixture fault gauge and the mass fraction of kaolinite.

Author contributions

DR: Conceptualization, Funding acquisition, Writing–original draft, Writing–review and editing.

Funding

Conflict of interest

The author declares that the research was conducted in the absence of any commercial or financial relationships that could be construed as a potential conflict of interest.

Publisher's note

All claims expressed in this article are solely those of the authors and do not necessarily represent those of their affiliated organizations, or those of the publisher, the editors and the reviewers. Any product that may be evaluated in this article, or claim that may be made by its manufacturer, is not guaranteed or endorsed by the publisher.

References

Adjemian, F., and Evesque, P. (2004). Experimental study of stick-slip behaviour. *Int. J. Numer. Anal. Methods Geomechanics* 28 (6), 501–530. doi:10.1002/nag.350

Albert, I., Tegzes, P., Albert, R., Sample, J. G., Barabási, A. L., Vicsek, T., et al. (2001). Stick-slip fluctuations in granular drag. *Phys. Rev. E* 64 (3), 031307. doi:10.1103/physreve.64.031307

Anthony, J. L., and Marone, C. (2005). Influence of particle characteristics on granular friction. *J. Geophys. Res. Solid Earth* 110 (B8). doi:10.1029/2004jb003399

Bedford, J., Faulkner, D., and Lapusta, N. (2022). Fault rock heterogeneity can produce fault weakness and reduce fault stability. *Nat. Commun.* 13, 326. doi:10.1038/s41467-022-27998-2

Bendavid, O., Cohen, G., and Fineberg, J. (2010). The dynamics of the onset of frictional slip. *Science* 330 (6001), 211–214. doi:10.1126/science.1194777

Brace, W. F., and Byerlee, J. D. (1966). Stick-slip as a mechanism for earthquakes. *Science* 153 (3739), 990–992. doi:10.1126/science.153.3739.990

Buijze, L., Guo, Y., Niemeijer, A. R., Ma, S., and Spiers, C. (2021). Effects of heterogeneous gouge segments on the slip behavior of experimental faults at dm scale. *Earth Planet. Sci. Lett.* 554, 116652. doi:10.1016/j.epsl.2020.116652

Byerlee, J. (1978). "Friction of rocks," in *Rock friction and earthquake prediction* (Basel: Birkhäuser), 615–626.

Chlieh, M., Avouac, J. P., Sieh, K., Natawidjaja, D. H., and Galetzka, J. (2008). Heterogeneous coupling of the sumatran megathrust constrained by geodetic and paleogeodetic measurements. *J. Geophys. Res. Solid Earth* 113. doi:10.1029/2007jb004981

de Meer, S., and Spiers, C. J. (1997). Uniaxial compaction creep of wet gypsum aggregates. *J.Geophys. Res. Solid Earth102 (B1)* 102, 875–891. doi:10.1029/96jb02481

Dieterich, J. H. (1979). Modeling of rock friction: 1. Experimental results and constitutive equations. *J. Geophys. Res.* 84 (B5), 2161–2168. doi:10.1029/jb084ib05p02161

Engelder, T. (1978). Aspects of asperity-surface interaction and surface damage of rocks during experimental frictional sliding. *pure Appl. Geophys.* 116 (4-5), 705–716. doi:10.1007/bf00876533

Freymueller, J. T., Cohen, S. C., and Fletcher, H. J. (2000). Spatial variations in present-day deformation, kenai peninsula, Alaska, and their implications. *J. Geophys. Res.* 105 (B4), 8079–8101. doi:10.1029/1999jb900388

Frye, K. M., and Marone, C. (2002). The effect of particle dimensionality on granular friction in laboratory shear zones. *Geophys. Res. Lett.* 29 (19), 22. doi:10.1029/2002gl015709

Géminard, J. C., Losert, W., and Gollub, J. P. (1999). Frictional mechanics of wet granular material. *Phys. Rev. E* 59 (5), 5881–5890. doi:10.1103/physreve.59.5881

Han, R., Hirose, T., Shimamoto, T., Lee, Y., and Ando, J. i. (2011). Granular nanoparticles lubricate faults during seismic slip. *Geology* 39 (6), 599–602. doi:10.1130/g31842.1

Härtl, J., and Ooi, J. Y. (2008). Experiments and simulations of direct shear tests: porosity, contact friction and bulk friction. *Granul. Matter* 10 (4), 263–271. doi:10.1007/s10035-008-0085-3

He, C., Ma, S., and Huang, J. (1998). Transition between stable sliding and stick-slip due to variation in slip rate under variable normal stress condition. *Geophys. Res. Lett.* 25 (17), 3235–3238. doi:10.1029/98gl02518

He, C., Wang, Z., and Yao, W. (2007). Frictional sliding of gabbro gouge under hydrothermal conditions. *Tectonophysics* 445 (3-4), 353–362. doi:10.1016/j.tecto.2007.09.008

Hedayat, A., Haeri, H., Hinton, J., Masoumi, H., and Spagnoli, G. (2018). Geophysical signatures of shear-induced damage and frictional processes on rock joints. *J. Geophys. Res. Solid Earth* 123 (2), 1143–1160. doi:10.1002/2017jb014773

Ikari, M. J., Niemeijer, A. R., and Marone, C. (2015). Experimental investigation of incipient shear failure in foliated rock. *J. Struct. Geol.* 77, 82–91. doi:10.1016/j.jsg.2015.05.012

Jiang, Y., Wang, G., Kamai, T., and McSaveney, M. J. (2016). Effect of particle size and shear speed on frictional instability in sheared granular materials during large shear displacement. *Eng. Geol.* 210, 93–102. doi:10.1016/j.enggeo.2016.06.005

Johnson, P. A., Ferdowsi, B., Kaproth, B. M., Scuderi, M., Griffa, M., Carmeliet, J., et al. (2013). Acoustic emission and microslip precursors to stick-slip failure in sheared granular material. *Geophys. Res. Lett.* 40 (21), 5627–5631. doi:10.1002/2013gl057848

Johnson, T., Wu, F. T., and Scholz, C. H. (1973). Source parameters for stick-slip and for earthquakes. *Science* 179 (4070), 278–280. doi:10.1126/science.179.4070.278

Johnson, T. L., and Scholz, C. H. (1976). Dynamic properties of stick-slip friction of rock. *J. Geophys. Res.* 81 (5), 881–888. doi:10.1029/jb081i005p00881

Kaproth, B. M., and Marone, C. (2013). Slow earthquakes, preseismic velocity changes, and the origin of slow frictional stick-slip. *Science* 341 (6151), 1229–1232. doi:10.1126/science.1239577

Karner, S. L., and Marone, C. (2000). Effects of loading rate and normal stress on stress drop and stick-slip recurrence interval. *Geophys. Monograph-American Geophys. Union* 120, 187–198. doi:10.1029/GM120p0187

Kato, N., Yamamoto, K., Yamamoto, H., and Hirasawa, T. (1992). Strain-rate effect on frictional strength and the slip nucleation process. *Tectonophysics* 211 (1-4), 269–282. doi:10.1016/0040-1951(92)90064-d

Lastakowski, H., Géminard, J. C., and Vidal, V. (2015). Granular friction: triggering large events with small vibrations. *Sci. Rep.* 5, 13455. doi:10.1038/srep13455

Leeman, J., Scuderi, M. M., Marone, C., and Saffer, D. (2015). Stiffness evolution of granular layers and the origin of repetitive, slow, stick-slip frictional sliding. *Granul. Matter* 17 (4), 447–457. doi:10.1007/s10035-015-0565-1

Lieou, C. K. C., Daub, E. G., Guyer, R. A., Ecke, R. E., Marone, C., and Johnson, P. A. (2017). Simulating stick-slip failure in a sheared granular layer using a physics-based constitutive model. *J. Geophys. Res. Solid Earth* 122 (1), 295–307. doi:10.1002/2016jb013627

Lockner, D. A., and Okubo, P. G. (1983). Measurements of frictional heating in granite. *J. Geophys. Res. Solid Earth* 88 (B5), 4313–4320. doi:10.1029/jb088ib05p04313

Lu, Z., and He, C. (2014). Frictional behavior of simulated biotite fault gouge under hydrothermal conditions. *Tectonophysics* 622, 62–80. doi:10.1016/j.tecto.2014.03.002

Mair, K., Frye, K. M., and Marone, C. (2002). Influence of grain characteristics on the friction of granular shear zones. *J. Geophys. Res. Solid Earth* 107 (B10), ECV 4-1. doi:10.1029/2001jb000516

Marone, C. (1998). Laboratory-derived friction laws and their application to seismic faulting. *Annu. Rev. Earth Planet. Sci.* 26 (1), 643–696. doi:10.1146/annurev.earth.26.1.643

Marone, C., Carpenter, B. M., and Schiffer, P. (2008). Transition from rolling to jamming in thin granular layers. *Phys. Rev. Lett.* 101 (24), 248001. doi:10.1103/physrevlett.101.248001

Moore, D. E., Lockner, D. A., Ma, S., Summers, R., and Byerlee, J. D. (1997). Strengths of serpentinite gouges at elevated temperatures. *J. Geophys. Res. Solid Earth* 102 (B7), 14787–14801. doi:10.1029/97jb00995

Morrow, C. A., and Byerlee, J. D. (1989). Experimental studies of compaction and dilatancy during frictional sliding on faults containing gouge. *J. Struct. Geol.* 11 (7), 815–825. doi:10.1016/0191-8141(89)90100-4

Niemeijer, A., Di Toro, G., Griffith, W. A., Bistacchi, A., Smith, S. A., and Nielsen, S. (2012). Inferring earthquake physics and chemistry using an integrated field and laboratory approach. *J. Struct. Geol.* 39 (0), 2–36. doi:10.1016/j.jsg.2012.02.018

Rivière, J., Lv, Z., Johnson, P. A., and Marone, C. (2018). Evolution of b-value during the seismic cycle: insights from laboratory experiments on simulated faults. *Earth Planet. Sci. Lett.* 482, 407–413. doi:10.1016/j.epsl.2017.11.036

Ruina, A. (1983). Slip instability and state variable friction laws. *J. Geophys. Res.* 88 (B12), 10359–10370. doi:10.1029/jb088ib12p10359

Sammis, C. G., and Biegel, R. L. (1989). Fractals, fault-gouge, and friction. *Pure Appl. Geophys.* 131 (1-2), 255–271. doi:10.1007/bf00874490

Scholz, C. H. (1989). The mechanics of earthquakes and faulting. *Geol. Curtain Engl. version* 17 (1), 49.

Scholz, C. H. (1998). Earthquakes and friction laws. *Nature* 391, 37–42. doi:10.1038/34097

Scholz, C. H., and Engelder, J. T. (1976). The role of asperity indentation and ploughing in rock friction—I: asperity creep and stick-slip. *International Journal of Rock Mechanics and Mining Sciences & Geomechanics Abstracts* 13 (5), 149–154. doi:10.1016/0148-9062(76)90819-6

Scuderi, M. M., Carpenter, B. M., Johnson, P. A., and Marone, C. (2015). Poromechanics of stick-slip frictional sliding and strength recovery on tectonic faults. *J. Geophys. Res. Solid Earth* 120 (10), 6895–6912. doi:10.1002/2015jb011983

Shinbrot, T., Kim, N. H., and Thyagu, N. N. (2012). Electrostatic precursors to granular slip events. *Proc. Natl. Acad. Sci.* 109 (27), 10806–10810. doi:10.1073/pnas.1121596109

Togo, T., Shimamoto, T., Ma, S., and Hirose, T. (2011). High-velocity frictional behavior of Longmenshan fault gouge from Hongkou outcrop and its implications for dynamic weakening of fault during the 2008 Wenchuan earthquake. *Earthq. Sci.* 24 (3), 267–281. doi:10.1007/s11589-011-0790-6

Tullis, T. E. (1988). Rock friction constitutive behavior from laboratory experiments and its implications for an earthquake prediction field monitoring program. *Pure Appl. Geophys.* 126 (2-4), 555–588. doi:10.1007/bf00879010

Weeks, J. D., and Tullis, T. E. (1985). Frictional sliding of dolomite: a variation in constitutive behavior. *J. Geophys. Res. Solid Earth* 90 (B9), 7821–7826. doi:10.1029/jb090ib09p07821

West, M., Sánchez, J. J., and Mcnutt, S. R. (2005). Periodically triggered seismicity at mount wrangell, Alaska, after the sumatra earthquake. *Science* 308 (5725), 1144–1146. doi:10.1126/science.1112462

Yao, L., Ma, S., Niemeijer, A. R., Shimamoto, T., and Platt, J. D. (2016). Is frictional heating needed to cause dramatic weakening of nanoparticle gouge during seismic slip? Insights from friction experiments with variable thermal evolutions. *Geophys. Res. Lett.* 43 (13), 6852–6860. doi:10.1002/2016gl069053